



Finite Volume for Fusion Simulations

Elise Estibals, Hervé Guillard, Afeintou Sangam

► To cite this version:

Elise Estibals, Hervé Guillard, Afeintou Sangam. Finite Volume for Fusion Simulations. Jorek Meeting 2016, Matthias Hoelzl, Apr 2016, Sophia Antipolis, France. hal-01397086

HAL Id: hal-01397086

<https://inria.hal.science/hal-01397086>

Submitted on 18 Nov 2016

HAL is a multi-disciplinary open access archive for the deposit and dissemination of scientific research documents, whether they are published or not. The documents may come from teaching and research institutions in France or abroad, or from public or private research centers.

L'archive ouverte pluridisciplinaire **HAL**, est destinée au dépôt et à la diffusion de documents scientifiques de niveau recherche, publiés ou non, émanant des établissements d'enseignement et de recherche français ou étrangers, des laboratoires publics ou privés.

Finite Volume for Fusion Simulations

E. Estibals H. Guillard A. Sangam
elise.estibals@inria.fr Inria Sophia Antipolis Méditerranée

November 15, 2016



Plan

1 MHD equations and issues

2 Free-divergence

- Well-known methods
- Vector potential
- Divergence cleaning methods
- Proposed method

3 Scheme with projection

- 2-D system
- Evolution step
- Scheme with projection

4 Numerical tests

- Brio-Wu
- Orszag-Tang
- Kelvin-Helmholtz instabilities
- Screw pinch equilibrium

Resistive MHD equations

- Non-conservative equations: $E^{hd} = \frac{p}{\gamma-1} + \frac{1}{2}\rho\mathbf{u}^2$,
 $\mathbf{E} = \mathbf{B} \times \mathbf{u} + \eta\mathbf{J}$

$$\begin{cases} \partial_t \rho + \nabla \cdot (\rho \mathbf{u}) &= 0, \\ \partial_t(\rho \mathbf{u}) + \nabla \cdot (\rho \mathbf{u} \otimes \mathbf{u}) + \nabla p &= \mathbf{J} \times \mathbf{B}, \\ \partial_t E^{hd} + \nabla \cdot [(E^{hd} + p)\mathbf{u}] &= (\mathbf{J} \times \mathbf{B}) \cdot \mathbf{u} + \eta \mathbf{J}^2, \\ \partial_t \mathbf{B} + \nabla \times \mathbf{E} &= 0. \end{cases}$$

- Conservative equations: $E = E^{hd} + \frac{1}{2}\mathbf{B}^2$, $p^* = p + \frac{1}{2}\mathbf{B}^2$

$$\begin{cases} \partial_t \rho + \nabla \cdot (\rho \mathbf{u}) &= 0, \\ \partial_t(\rho \mathbf{u}) + \nabla \cdot (\rho \mathbf{u} \otimes \mathbf{u} - \mathbf{B} \otimes \mathbf{B}) + \nabla p^* &= 0, \\ \partial_t E + \nabla \cdot [(E + p^*)\mathbf{u} - (\mathbf{u} \cdot \mathbf{B})\mathbf{B}] &= -\nabla \cdot (\eta \mathbf{J} \times \mathbf{B}), \\ \partial_t \mathbf{B} + \nabla \cdot (\mathbf{u} \otimes \mathbf{B} - \mathbf{B} \otimes \mathbf{u}) &= -\nabla(\eta \mathbf{J}). \end{cases}$$

MHD system

- Hyperbolic part of the system: 3 wave types
 - 2 Alfvén waves,
 - 4 magneto-acoustic waves (2 fast and 2 slow),
 - 2 material waves (moving with \mathbf{u}).
- Involution equation:

$$\partial_t(\nabla \cdot \mathbf{B}) = 0.$$

Then

$$\nabla \cdot \mathbf{B}(t=0) = 0 \Rightarrow \nabla \cdot \mathbf{B}(t) = 0 \quad \forall t.$$

- Numerical issues:
 - ① Shock capturing: need a robust and accurate scheme.
 - ② Free-divergence constraint.
 - ③ Time scale $T \gg T_{\text{alfven}} = L/v_{\text{alfven}}$: need implicit scheme.

Free-divergence constraint: Well-known methods

2 families of methods:

- Vector potential \mathbf{A} :

$$\mathbf{B} = \nabla \times \mathbf{A}.$$

- Divergence cleaning methods:

$$\text{Enforce } \nabla \cdot \mathbf{B} = 0.$$

Vector potential **A**

Replace **B** by **A** in the equation:

$$\partial_t \mathbf{A} - \mathbf{u} \times (\nabla \times \mathbf{A}) + \eta \nabla \times (\nabla \times \mathbf{A}) = -\nabla U.$$

Advantage:

- Insure $\nabla \cdot \mathbf{B} = 0$.

Drawbacks:

- One order higher in the spatial derivatives.
- More complex system of equation.

Divergence cleaning methods: Previous works

- Powell et al. (JCP, 1999): Add a source term proportionnal to $\nabla \cdot \mathbf{B}$.

$$\partial_t \mathbf{B} + \nabla \cdot (\mathbf{u} \otimes \mathbf{B} - \mathbf{B} \otimes \mathbf{u}) = -(\nabla \cdot \mathbf{B})\mathbf{u}.$$

- Munz et al. (JCP, 2000), Dedner et al. (JCP, 2001): Generalized Lagrange Multiplier (GLM) method.

$$\begin{aligned}\partial_t \mathbf{B} + \nabla \cdot (\mathbf{u} \otimes \mathbf{B} - \mathbf{B} \otimes \mathbf{u}) + \nabla \Psi &= 0, \\ \mathcal{D}(\Psi) + \nabla \cdot \mathbf{B} &= 0, \\ \mathcal{D}(\Psi) &= \frac{1}{c_h^2} \partial_t \Psi + \frac{1}{c_p^2} \Psi.\end{aligned}$$

- Balsara and Spicer (JCP, 1998): Constrained transport method.

$$\frac{d}{dt} \int_{\mathcal{S}} \mathbf{B} \cdot d\mathcal{S} = - \oint_{\partial\mathcal{S}} \mathbf{E} \cdot d\mathbf{l}.$$

Divergence cleaning methods

Advantages:

- Easily incorporated with a Riemann type scheme.

Drawbacks:

- Divergence cleaning:
 - $\nabla \cdot \mathbf{B}$ appears in several equations.
 - Not approximated with the same discretization.
 - Divergence cleaning method insure $\nabla \cdot \mathbf{B} = 0$ for one discrete approximation.
- Constrained transport: difficult to implement for arbitrary meshes.

Proposed method

- A mixture of the two methods.
- Idea: work with a redundant system.
- Both vector potential and magnetic fields equations.
- Based on the relaxation scheme method:
 - ① Evolution step: FV method for all the variables.
 - ② Projection step: enforce $\mathbf{B} = \nabla \times \mathbf{A}$.

2-D implementation

- Scalar potential ψ :

$$\mathbf{B} = B_z \mathbf{e}_z + \mathbf{e}_z \times \nabla \psi.$$

- Augmented system:

$$\left\{ \begin{array}{lcl} \partial_t \rho + \nabla \cdot (\rho \mathbf{u}) & = & 0, \\ \partial_t (\rho \mathbf{u}) + \nabla \cdot (\rho \mathbf{u} \otimes \mathbf{u} - \mathbf{B} \otimes \mathbf{B}) + \nabla p^* & = & 0, \\ \partial_t E + \nabla \cdot [(E + p^*) \mathbf{u} - (\mathbf{u} \cdot \mathbf{B}) \mathbf{B}] & = & -\eta \nabla \cdot (\mathbf{J} \times \mathbf{B}), \\ \partial_t \mathbf{B} + \nabla \cdot (\mathbf{u} \otimes \mathbf{B} - \mathbf{B} \otimes \mathbf{u}) & = & \eta \nabla^2 \mathbf{B}, \\ \partial_t \psi + \mathbf{u} \cdot \nabla \psi & = & \eta \nabla^2 \psi. \end{array} \right.$$

Evolution step

- System $\partial_t U + \partial_x F(U) + \partial_y G(U) = 0$:

$$U_{i,j}^{n+1} = U_{i,j}^n - \frac{\Delta t}{\Delta x} (F_{i+1/2,j} - F_{i-1/2,j}) - \frac{\Delta t}{\Delta y} (G_{i,j+1/2} - G_{i,j-1/2}).$$

- $F_{i+1/2,j}$ and $G_{i,j+1/2}$ computed with a Riemann solver.

Evolution step: HLLD scheme

- Miyoshi and Kusano (JCP, 2005).
- Approximate Riemann solver with 4 intermediate states.

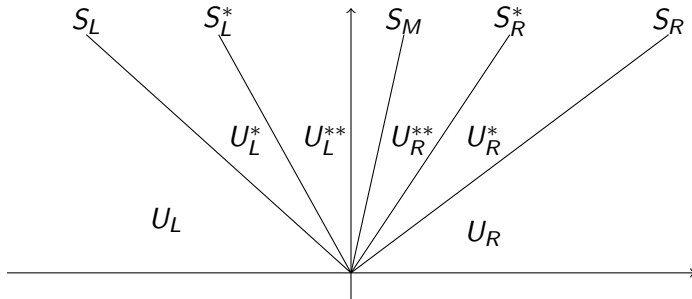


Figure : Riemann fan with four intermediate states.

Evolution step: HLLD scheme

- Intermediate fluxes:

$$\begin{cases} F_K^* = F_K + S_K U_K^* - S_K U_K \\ F_K^{**} = F_K + S_K^* U_K^{**} - (S_K^* - S_K) U_K^* - S_K U_K \end{cases}, K = L, R.$$

- $\rho\psi$ flux:

$$F(\rho\psi) = F(\rho) \times \begin{cases} \psi_L, & 0 \leq S_M \\ \psi_R, & 0 \geq S_M \end{cases}.$$

Scheme with projection

① Evolution step: HLLD scheme

$$\begin{cases} \mathbf{B}_{i,j}^{n+1/2}, \\ \psi_{i,j}^{n+1/2}. \end{cases}$$

② Projection step:

$$\begin{cases} \psi_{i,j}^{n+1} = \psi_{i,j}^{n+1/2}, \\ \mathbf{B}_{i,j}^{n+1} = B_{z,i,j}^{n+1/2} \mathbf{e}_z + \mathbf{e}_z \times (\nabla \psi)_{i,j}^{n+1}. \end{cases}$$

Numerical tests

Shock capturing tests:

- Brio-Wu,
- Orszag-Tang,
- Kelvin-Helmholtz.

Plasma fusion tests:

- Screw pinch equilibrium.

1-D Brio-Wu shock tube

- Magnetic field:

$$\mathbf{B} = B_x \mathbf{e}_x + \partial_x \psi \mathbf{e}_y.$$

- 1-D equation for the potential ψ :

$$\partial_t(\rho\psi) + \partial_x(\rho\psi u) = B_x \rho v.$$

- Initial conditions:

	ρ	\mathbf{u}	p	B_x	$B_y = \partial_x \psi$	ψ
$x < 0.5$	1	0	1	0.75	1	x
$x > 0.5$	0.125	0	0.1	0.75	-1	$1 - x$

- 1-D mesh: 100 points
- Final time: 0.1

1-D Brio-Wu: Magnetic component B_y

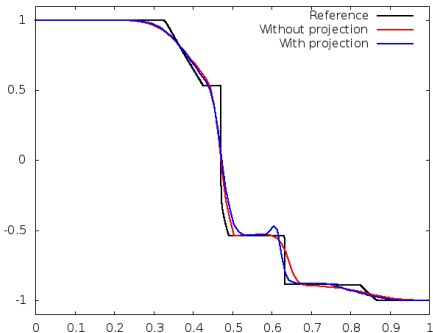


Figure : HLLD O(1).

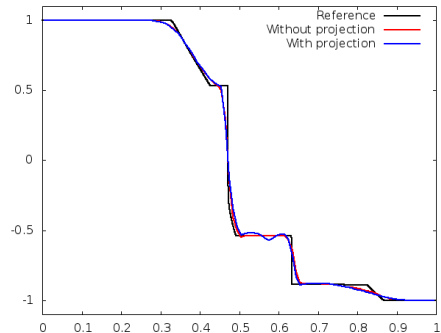


Figure : HLLD O(2).

2-D Brio-Wu shock tube

- Potential:

$$\psi(x, y) = \begin{cases} x - 0.75y, & x < 0.5 \\ 1 - x - 0.75y, & x > 0.5 \end{cases}.$$

- 2-D mesh: 100×10 cells.

2-D Brio-Wu shock tube

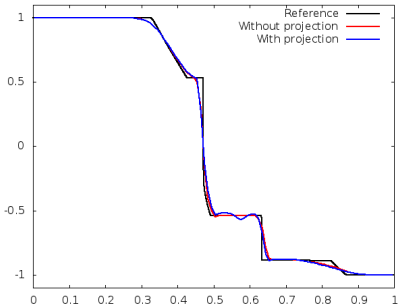


Figure : B_y HLLD O(2).

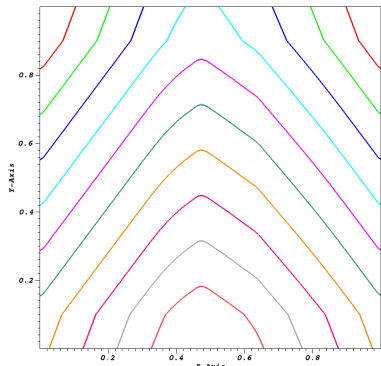


Figure : ψ , HLLD O(2).

Orszag-Tang

- Initial conditions: $\gamma = 5/3$

ρ	$u(x, y)$	$v(x, y)$	$p(x, y)$	$B_x(x, y)$	$B_y(x, y)$	$\psi(x, y)$
γ^2	$-\sin(2\pi y)$	$\sin(2\pi x)$	γ	$-\sin(2\pi y)$	$\sin(4\pi x)$	$-\frac{1}{2\pi} \cos(2\pi y) - \frac{1}{4\pi} \cos(4\pi x)$

- Mesh: 512×512 cells.
- Final time: 0.5.

Orszag-Tang: Pressure field

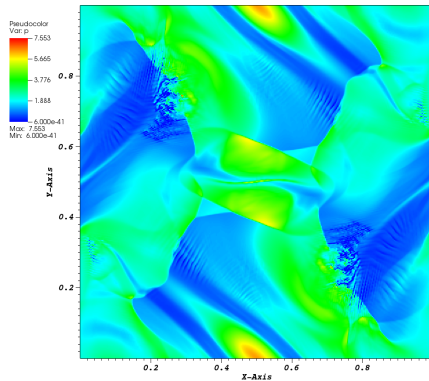


Figure : Without projection.

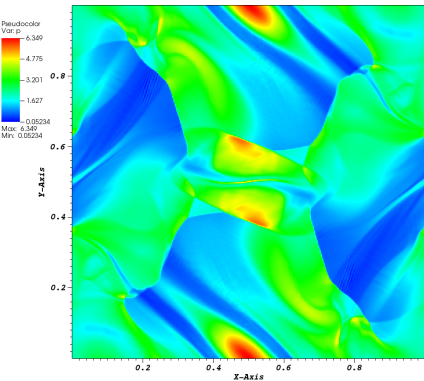


Figure : With projection.

Orszag-Tang

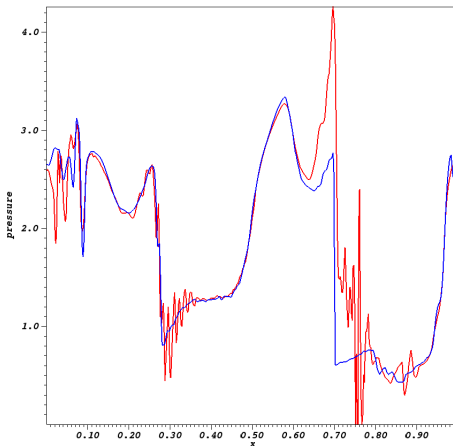


Figure : Pressure at $y = 0.3125$ Red: without projection, Blue: with projection.

Orszag-Tang

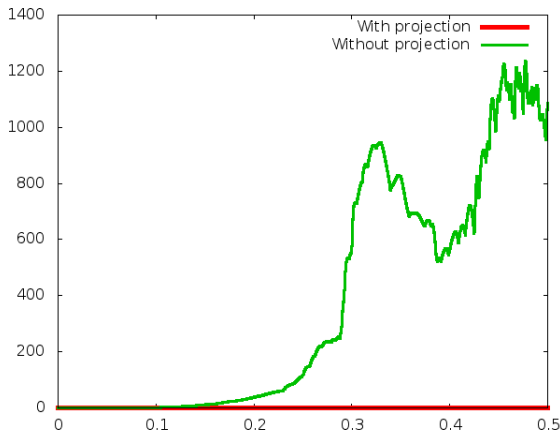


Figure : $\|\nabla \cdot \mathbf{B}\|_\infty$.

Kelvin-Helmholtz instabilities

- Initial data

ρ	p	$u(x, y)$	$v(x, y)$	$B_x(x, y)$	$B_y(x, y)$	$B_z(x, y)$	$\psi(x, y)$
1	$\frac{1}{\gamma}$	$\frac{1}{2} \tanh(\frac{y}{y_0})$	0	$0.1 \cos(\frac{\pi}{3}) \sqrt{\rho}$	0	$0.1 \sin(\frac{\pi}{3}) \sqrt{\rho}$	$-0.1 \cos(\frac{\pi}{3}) \sqrt{\rho} y$

- Single mode perturbation

$$v(x, y) = 0.01 \sin(2\pi x) \exp(-\frac{y^2}{\sigma^2}), \quad \sigma = 0.01.$$

- Mesh: 256×512 points

$$\frac{B_{pol}}{B_{tor}} = \frac{\sqrt{B_x^2 + B_y^2}}{B_z}.$$

Kelvin-Helmholtz: $t = 5.0$

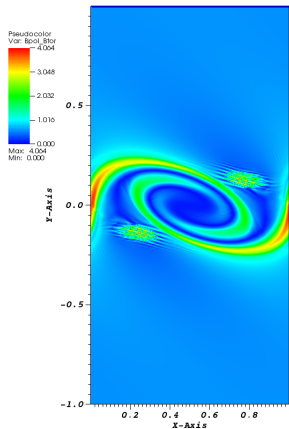


Figure : Without projection.

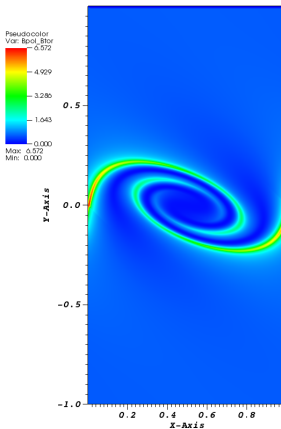


Figure : With projection.

Kelvin-Helmholtz: $t = 8.0$

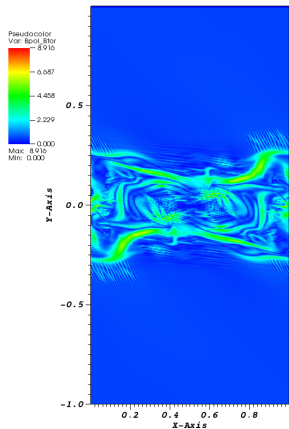


Figure : Without projection.

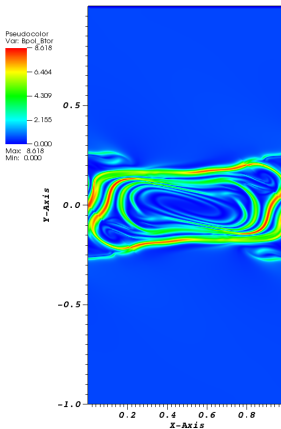


Figure : With projection.

Kelvin-Helmholtz: $t = 12.0$

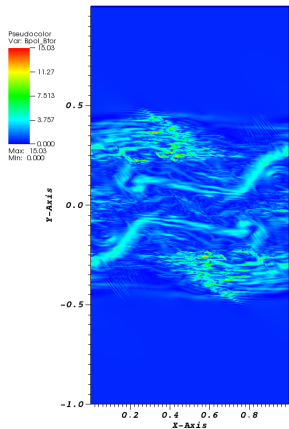


Figure : Without projection.

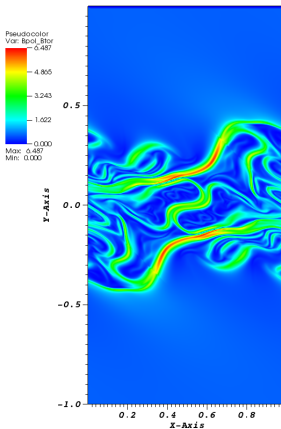


Figure : With projection.

Kelvin-Helmholtz: $t = 20.0$

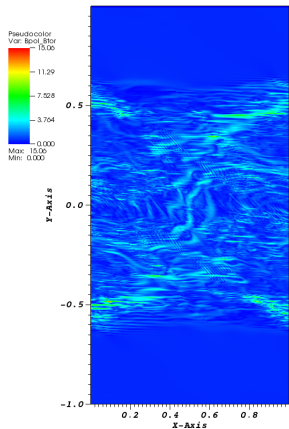


Figure : Without projection.

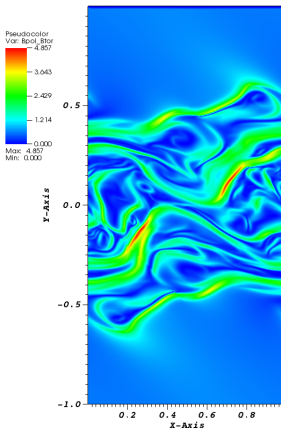


Figure : With projection.

Kelvin-Helmholtz

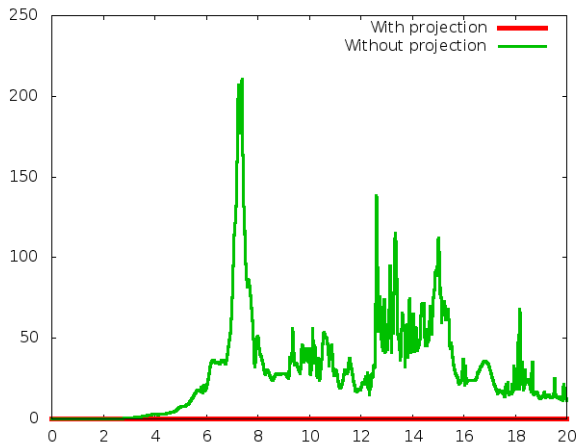


Figure : $\|\nabla \cdot \mathbf{B}\|_\infty$.

Preliminary test for fusion plasma

- Equilibrium computation: $\nabla p = \mathbf{J} \times \mathbf{B}$.
- Initial conditions:

$$\begin{cases} R_0 = 10, & B_r = 0, \\ \rho = 1, & B_\theta(r) = \frac{r}{R_0(3r^2+1)}, \\ \mathbf{u} = 0, & B_z = 1, \\ p(r) = \frac{1}{6R_0^2(3r^2+1)^2}, & \psi(r) = \frac{1}{6R_0} \ln(3r^2 + 1). \end{cases}$$

- Aligned mesh: cylindrical coordinates (100×10 cells).
- Non aligned mesh: Cartesian coordinates (200×200 cells).

Cylindrical coordinates

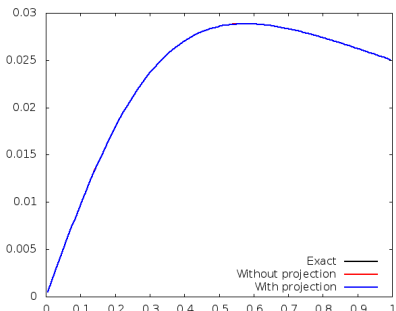


Figure : B_θ .

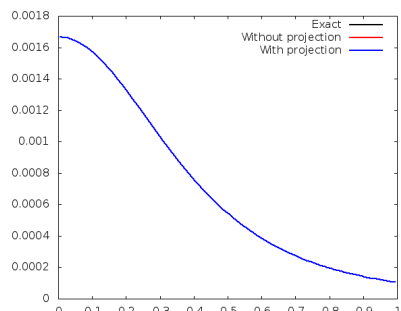


Figure : p .

Cylindrical coordinates: steady state

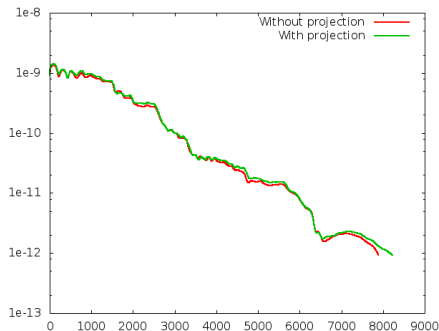


Figure : Residual on r -momentum equation.

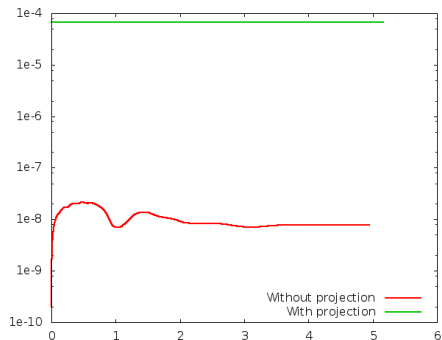


Figure : Relative error of B_θ .

Cartesian coordinates

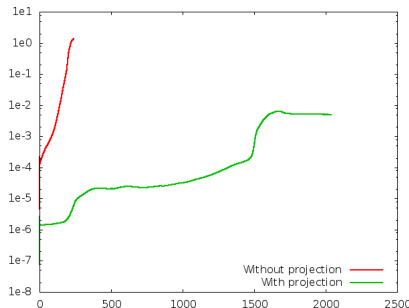
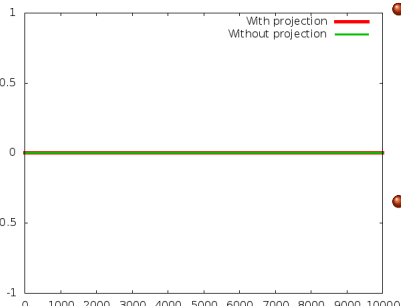


Figure : Relative error of p in function of Alfvén time.

- Non aligned meshes: with projection simulations maintains the equilibrium on 1000 Alfvén times (around $0.5ms$ and 10^6 time steps).
- However, we want to perform the simulation on several milliseconds.

Remedies



- A simple trick: remove the truncation error evaluated at time $t = 0$.
- $$\partial_t(\rho \mathbf{u}) + \nabla \cdot (\rho \mathbf{u} \otimes \mathbf{u}) + \nabla p - \mathbf{J} \times \mathbf{B} - (\nabla_h p - \mathbf{J}_h \times \mathbf{B}_h)_{eq} = 0.$$
- Well-balanced scheme: work in progress.

Figure : Relative error of p .

Conclusions and perspectives

Conclusions:

- Shock capturing tests: Scheme with projection gives satisfactory results.
- Plasma fusion test: Work in progress on well-balanced scheme.

Perspectives:

- Perform more tests for plasma fusion (kink instability).
- Adapt to 3-D geometry.
- Test on resistive problems.

Cylindrical equations

$$\left\{ \begin{array}{lcl} \partial_t(r\rho) + \partial_r(r\rho u_r) + \partial_\theta(\rho u_\theta) & = & 0, \\ \partial_t(r\rho u_r) + \partial_r[r(\rho u_r^2 + p^* - B_r^2)] + \partial_\theta(\rho u_r u_\theta - B_r B_\theta) & = & \rho u_\theta^2 + p^* - B_\theta^2, \\ \partial_t(r^2\rho u_\theta) + \partial_r[r^2(\rho u_r u_\theta - B_r B_\theta)] + \partial_\theta[r(\rho u_\theta^2 + p^* - B_\theta^2)] & = & 0, \\ \partial_t(r\rho u_z) + \partial_r[r(\rho u_r u_z - B_r B_z)] + \partial_\theta(\rho u_\theta u_z - B_\theta B_z) & = & 0, \\ \partial_t(rE) + \partial_r[r[(E + p^*)u_r - (\mathbf{u} \cdot \mathbf{B})B_r]] + \partial_\theta[(E + p^*)u_\theta - (\mathbf{u} \cdot \mathbf{B})B_\theta] & = & 0, \\ \partial_t(rB_r) + \partial_\theta(u_\theta B_r - u_r B_\theta) & = & 0, \\ \partial_t B_\theta + \partial_r(u_r B_\theta - u_\theta B_r) & = & 0, \\ \partial_t(rB_z) + \partial_r[r(u_r B_z - u_z B_r)] + \partial_\theta(u_\theta B_z - u_z B_\theta) & = & 0, \\ \partial_t(r\rho\psi) + \partial_r(r\rho\psi u_r) + \partial_\theta(\rho\psi u_\theta) & = & 0. \end{array} \right.$$

Scheme with projection

① Evolution step: HLLD scheme

$$\left\{ \begin{array}{l} p_{i,j}^{n+1/2}, \\ \mathbf{B}_{i,j}^{n+1/2}, \\ \psi_{i,j}^{n+1/2}. \end{array} \right.$$

② Projection step:

$$\left\{ \begin{array}{lcl} \psi_{i,j}^{n+1} & = & \psi_{i,j}^{n+1/2}, \\ \mathbf{B}_{i,j}^{n+1} & = & B_{z,i,j}^{n+1/2} \mathbf{e}_z + \mathbf{e}_z \times (\nabla \psi)_{i,j}^{n+1}, \\ E_{i,j}^{n+1} & = & \frac{p_{i,j}}{\gamma-1} + \frac{1}{2} \rho^{n+1/2} \mathbf{u}^2 + \frac{1}{2} (\mathbf{B}_{i,j}^{n+1})^2. \end{array} \right.$$